Design and Integration of a Reconfiguration Robot

Jun Jiang, Houde Liu(✉), Bo Yuan, Lunfei Liang, and Bin Liang

Graduate School at Shenzhen, Tsinghua University,
Shenzhen 518055, People's Republic of China
{jiang.jun,liu.hd}@sz.tsinghua.edu.cn

Abstract. Based on the kinematic topology of bionic robot and robot motion planning modeling, this paper designs the mechanical structure of highly integrated robotic joint module, the fast self-reconfigurable module, the drive control software, and the hardware for the system. Through the experimental verification and simulation data analysis, the robot joint module and the fast self-reconfiguration module designed in this paper meet the performance requirement of the reconfigurable intelligent robot. Finally, the prototype verification of the reconfigurable intelligent robot is realized in this paper.

Keywords: Reconfigurable robot · Joint module · Reconfiguration module

1 Introduction

In the early 1990s, researchers proposed a recombination system based on chain structure [1] and dot matrix format [2], on which the future development trend of modular robots were based. Subsequently, self-reconfigurable robots have been greatly developed in countries around the world, and Japan and the United States have developed most rapidly in this regard. Some universities and research institutions [3–8] in the United States and Japan have conducted extensive and in-depth research on reconstruction techniques, deformation strategies, motion planning, control algorithms, architecture, and collaborative control of reconstructed robots. The reconstruction method of the robot also evolved from the initial static reconfigurable method to the dynamic self-reconfiguration method, and established a variety of model experiment systems. This research has made great progress both in technology and in performance.

In addition, the controller and the driver are embedded in the joint module with the internal wiring, that is used to obtain a modular joint module with light weight, large load-to-weight ratio, and low power consumption. As the core component of the robot, the modular joint module uses a quick connection mechanism for easy maintenance and robot configuration changes.

Therefore, this paper studies the design of the joint module that constitutes the necessary components of the robot, the quickly carried out the self-reconstruction module between the joint modules, and the corresponding drive controller that can realize the motion control of the joint module. Through the corresponding gait simulation analysis and research, this paper completed the design and integration of reconfigurable intelligent robots.

H. Yu et al. (Eds.): ICIRA 2019, LNAI 11742, pp. 339–350, 2019.
https://doi.org/10.1007/978-3-030-27535-8_31

2 Reconfigurable Intelligent Robot Overall Design

The overall system of the reconfigurable intelligent robot mainly includes the robot joint module, the fast self-reconfiguration module, the drive controller, and the central control system. The main functions of these four parts are as follows.

The robot joint module is mainly used to construct the robot body shape, and configure the appropriate motion freedom to facilitate the robot to walk or fine manipulation. The rapid self-reconfiguration module is mainly used to realize the reconfigurable transformation mode of the robot, and to realize more possible manipulation of the robot by expanding the degree of freedom of the robot arm. The drive controller is mainly used to realize the motion control of the robot joint module and rapid self-reconfiguration module, and communicate with the robot central controller. The robot central controller mainly realizes robot motion planning, motion pattern and motion mode, and controls the robot intelligent reconfigurable according to the requirements.

3 Design of Important Parts of Reconfigurable Robot

3.1 Reconfigurable Intelligent Robot Topology

According to different bionic objects, the bionic quadruped robot can be generally divided into mammalian robots [9], reptile robots [10] and insect animal robots [11], as shown in Fig. 1. The quadruped reptile and insect animal robots have lower center of gravity and higher stability. However, these two types of robots require large joint torque to bear their own weight and therefore have poor load capacity. But, the legs of the quadruped mammal are basically under the torso, which has a strong load capacity, can load heavier cargo and can move forward at a faster speed, and the stability control stability is also higher. In view of the advantages of quadruped mammalian robots in terms of weight and flexibility, this paper will focus on the study of reconfigurable intelligent robots in the form of quadruped mammals.

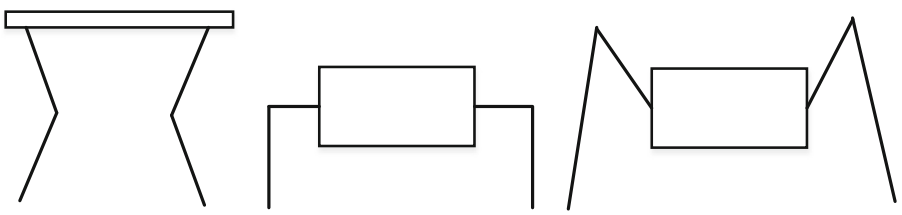

(a) Bionic quadruped mammalian (b) Bionic quadruped reptile robots (c) Bionic quadruped insect animal robot

Fig. 1. Bionic quadruped robot topology.

The reconfigurable intelligent robot three-dimensional model designed in this paper is shown in Fig. 2. The robot adopts a symmetrical regular quadrilateral arrangement. Each leg is evenly distributed around the body and has three rotational degrees of freedom. The foot end has a passive cushioning mechanism and a six-dimensional force sensor used to measure the change of the foot end force during the walking of the quadruped robot.

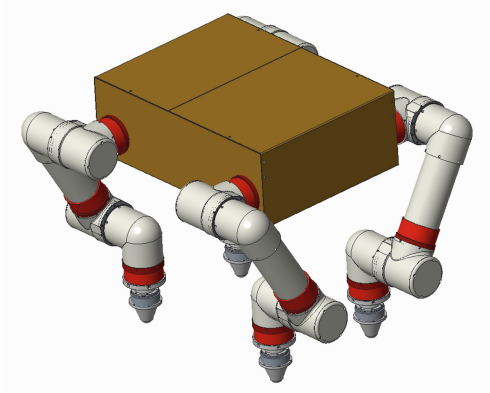

Fig. 2. The three-dimensional model of the reconfigurable robot

3.2 Reconfigurable Intelligent Robot Kinematics Modeling

At present, the methods of kinematics modeling of quadruped robots include D-H method [12], Lie algebra method [13] and spiral theory [14]. Among them, the D-H method is a more common method, which can solve the forward kinematics problem of a series mechanism with arbitrary degrees of freedom. In view of the fact that the reconfigurable intelligent robot has only three degrees of freedom in one leg, it is suitable to establish the kinematic equation of the robot by D-H method. In addition, since the four legs of the reconfigurable intelligent robot are identical in structure, it is only required to solve the kinematic equation of one leg. As shown in Fig. 3, it is a three-dimensional model diagram of one leg and a corresponding coordinate system.

The one-legged D-H kinematics model was established according to the Craig method [15]. The D-H parameters are shown in Table 1.

Table 1. D-H parameters of one-leg.

Joint j	$\alpha_{j-1}/(^\circ)$	$a_{j-1}/(\text{mm})$	$d_j/(\text{mm})$	$\theta_j/(^\circ)$
1	0	0	87	$\theta_1^{(i)} - 90$
2	−90	0	107	$\theta_2^{(i)}$
3	0	260.3	−107	$\theta_3^{(i)}$

In Table 1, α, a, and d is the torsion angle, length, and offset distance of joint connecting rod, respectively, and θ is the joint angle.

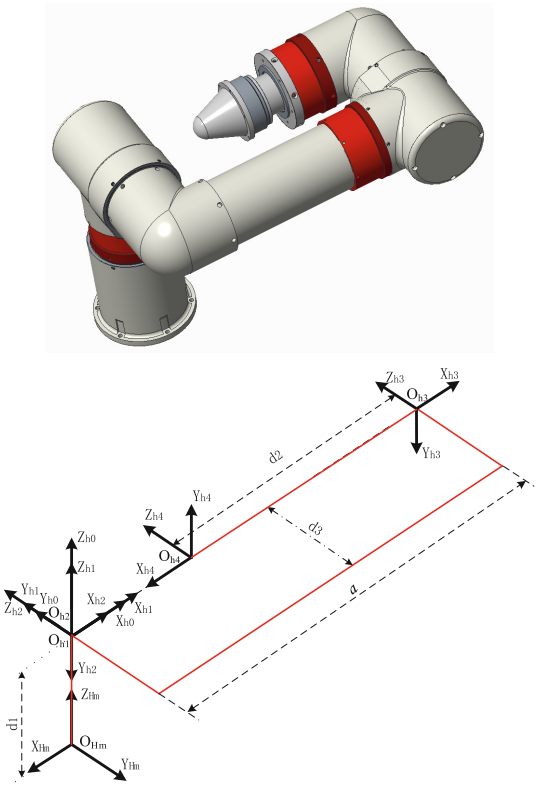

Fig. 3. Three-dimensional model diagram of one leg and a corresponding coordinate system

Based on one-legged kinematic D-H parameters of the quadruped robot, this paper establishes the positive kinematics model on it. The transformation matrix of the quadruped robot joint established by the D-H parameter method is as shown in the formula (1).

$$
{}_{j}^{j-1}T = \begin{bmatrix} \cos\theta_j & \cos\theta_j - \sin\theta_j & 0 & a_{j-1} \\ \sin\theta_j \cos\theta_{j-1} & \cos\theta_j \cos\alpha_{j-1} & -\sin\alpha_{j-1} & -\sin\alpha_{j-1} d_j \\ \sin\theta_j \sin\alpha_{j-1} & \cos\theta_j \sin\alpha_{j-1} & \cos\alpha_{j-1} & \cos\alpha_{j-1} d_j \\ 0 & 0 & 0 & 1 \end{bmatrix} \tag{1}
$$

In formula (1), ${}_{j}^{j-1}T$ represents the coordinate transformation matrix from joint $j-1$ to joint j. By substituting the D-H parameters of each joint in Table 1 into formula (1), the transformation matrix of each joint can be obtained.

3.3 Design of Reconfigurable Intelligent Robot Joint Module

This paper presents a highly integrated modular joint design. The joint adopts the hollow wire routing mode, the driving mechanism is a DC brushless motor [16], and the harmonic reducer [17] is used as the transmission mechanism to increase the output torque and has a strong load capacity. The joint has a wealth of sensor resources with greater precision, and has better environmental adaptability. In addition, a motion control driver is integrated inside the joint, and the overall structural composition of the joint is shown in Fig. 4.

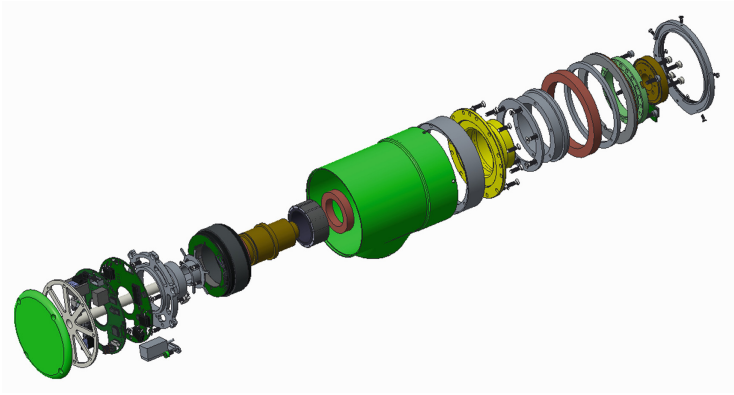

Fig. 4. The design drawing of reconfigurable intelligent robot joint module

3.4 Design of Fast Self-reconfigurable Module

The fast self-reconfigurable module interface adopts permanent magnet connection technology [18], and realizes power-off locking and power-on disconnection. So, this paper adopts plug and socket design, as shown in Fig. 5. Both the plug and the socket are designed with a large tolerance cone angle structure to facilitate connection and separation of the interface. The mating section of the plug and socket is designed with a spline-like structure for transmitting torque. The outer surface of the plug and the inner surface of the socket are provided with elastic electrical connecting sheets. When the plug is inserted into the socket, the elastic electrical connecting sheet is deformed to generate sufficient contact stress and contact area to form a reliable electrical connection. The plug and the socket are connected to the joint module through the connecting flange.

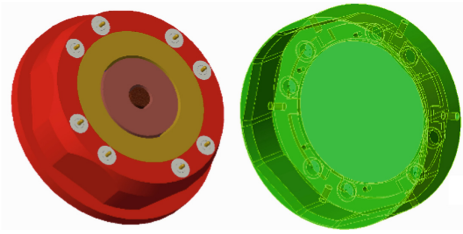

Fig. 5. The plug and socket of the fast self-reconfigurable module

3.5 Drive Controller Hardware Design of the Joint

In this paper, the drive controller is designed for joint module and self-reconfiguration module of the reconfigurable intelligent robot. The main functions of the drive controller include emergency brake enable, self-reconfiguration mechanism control and joint motor drive.

The drive controller system solution consists of two parts: the control board and the drive board. The control board adopts a processor [19] with an ARM core as the main control unit, executes the control commands from the host computer, collects the data information of various sensors, realizes the drive control and emergency braking of the servo motor, and controls self-reconfigurable module. The drive board mainly implements the power conversion function and completes the drive enable of the servo motor, as well as the functions of current acquisition and temperature acquisition.

Figure 6 shows the block diagram of the design of the reconfigurable intelligent robot drive controller.

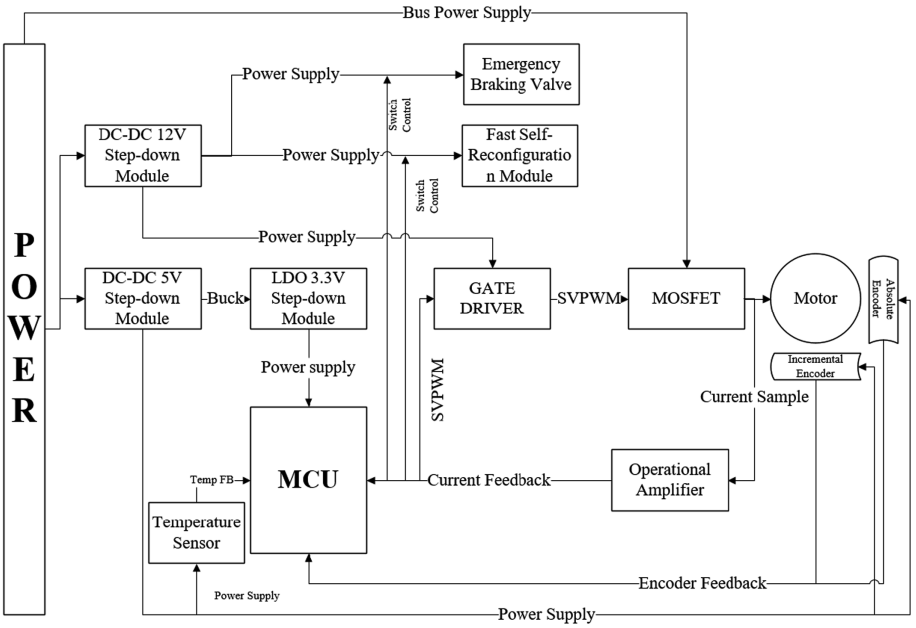

Fig. 6. The block diagram of the drive controller design

3.6 Drive Controller Software Design of the Joint

In this paper, a software system is designed for the hardware system of the robot joint module and the fast self-reconfiguration module, and ensures them can work safely and efficiently. After the entire software solution is powered on, the initialization operation is completed. Under normal circumstances, it is completely controlled by the upper

computer, and the operation command can be executed only after receiving the instruction of the upper computer. The flow chart of the entire system is shown in Fig. 7.

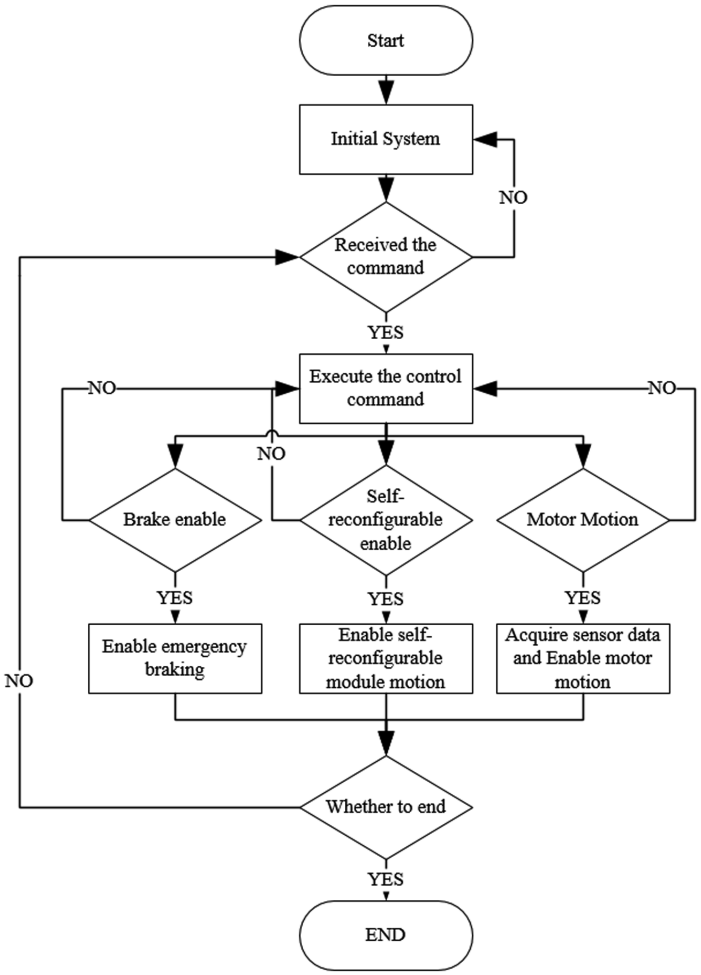

Fig. 7. The flow chart of the drive controller software design of the joint

4 Simulation and Verification

This paper studies the motion planning of the reconfigurable intelligent robot and uses the robot three-point gait method [20] to verify the performance of the reconfigurable intelligent robot. The three-point gait is a slow, static steady motion gait, suitable for motion in complex terrain environments, such as stairs, ruins, and other terrains with large undulating obstacles. In the face of this environment, the robot can swing at most

one leg at any time, and at least three legs are supported simultaneously. So there is always a support domain during the movement, so that the quadruped robot can maintain static stability.

According to the gait characteristics, one gait cycle can be divided into eight state phases: front left leg swing phase, transition support phase, hind right leg swing phase, transition support phase, front right leg swing phase, transition support phase, hind left leg swing phase, transition support phase. In here, the algorithm introduces a state machine based on a combination of time triggering and event triggering for gait control. In the single-leg swing phase, the swing leg landing triggers the next state phase; in the transitional support phase, the time of the currently planned transitional support phase triggers the next state phase. The control system real-time monitors the state of each leg of the reconfigurable robot, and outputs the state phase control signal according to the state transition.

4.1 Simulation Results of the Robot Three-Point Gait

In this paper, the dynamic simulation of the single-step motion time of the robot is 0.8 s by performing three-point gait simulation on the reconfiguration intelligent robot. The output of this simulation including joint position, joint speed, and joint torque, and the results are as follows.

Simulation Results of the Robot Joint Position

The simulation results are shown in Fig. 8, the root joint motion range is $-16.331 \sim 15.896°$, the hip joint motion range is $-20.324 \sim 57.215°$, and the knee joint motion range is $-101.387 \sim -24.263°$.

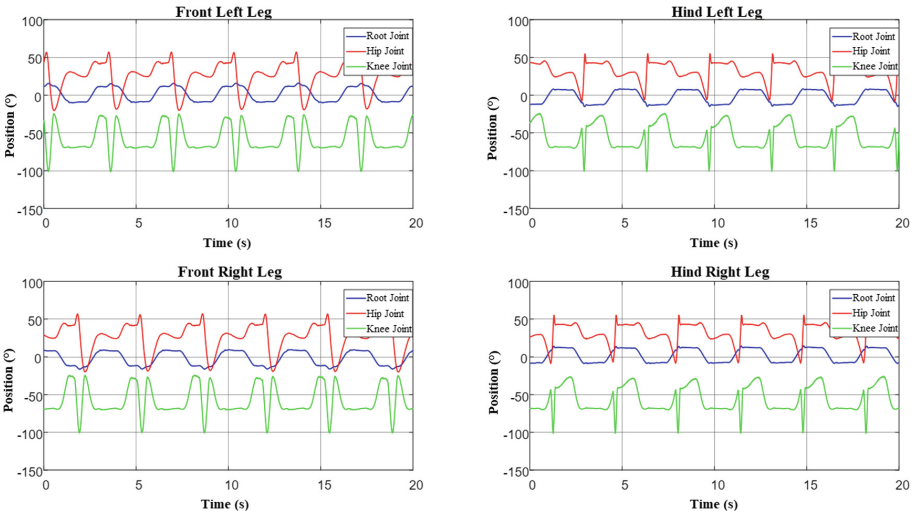

Fig. 8. The position curve of the robot joint

Simulation Results of the Robot Joint Speed

The simulation results are shown in Fig. 9, the maximum speed of the root joint, the hip joint, and the knee joint is 40.551°/s, 312.924°/s, and 412.605°/s, respectively.

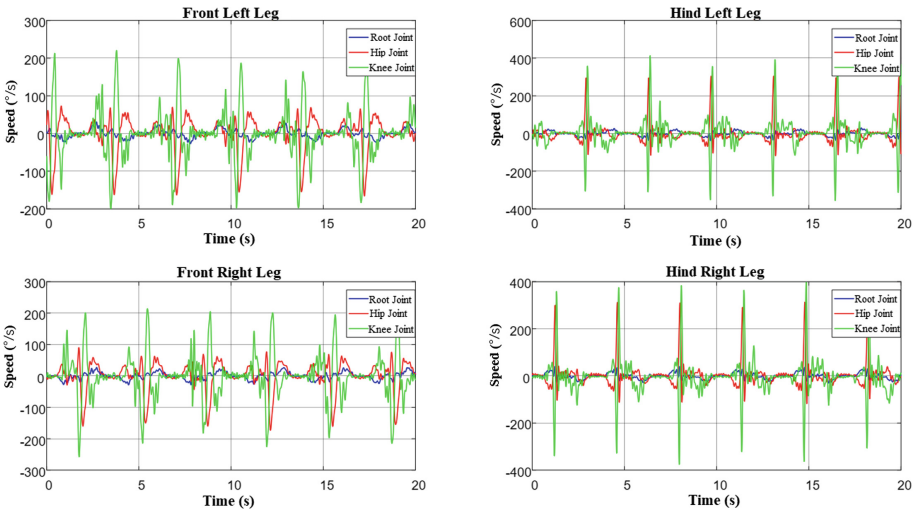

Fig. 9. The speed curve of the robot joint

Simulation Results of the Robot Joint Torque

The simulation results are shown in Fig. 10, the maximum torque of the root joint, the hip joint, and the knee joint are 28.947 Nm, 31.211 Nm, and 39.327 Nm, respectively.

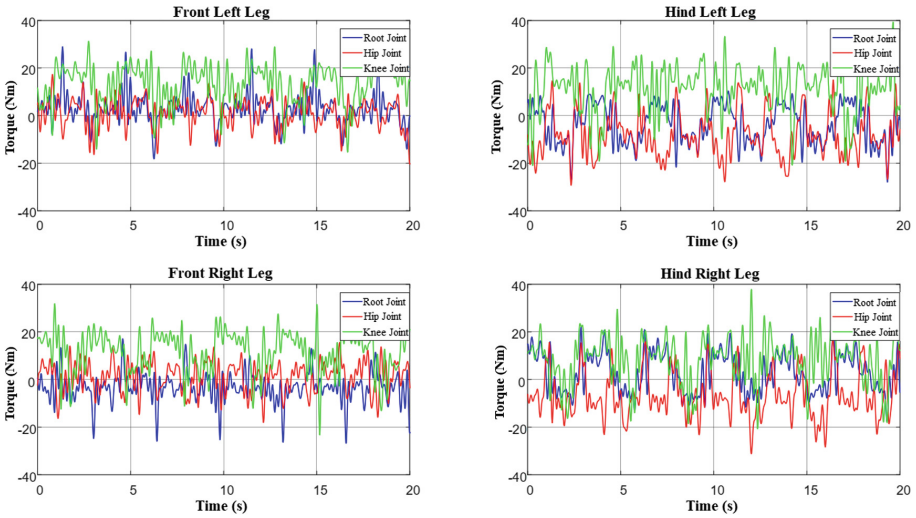

Fig. 10. The torque curve of the robot joint

4.2 The Test Results of the Joint of the Reconfigurable Intelligent Robot

The joint module designed in this paper can realize single-circle 360° position detection, maximum 3850 RPM speed operation, and 49 NM torque output. Figure 11 shows the speed, position and current feedback curves of the single joint under maximum load conditions during the actual test.

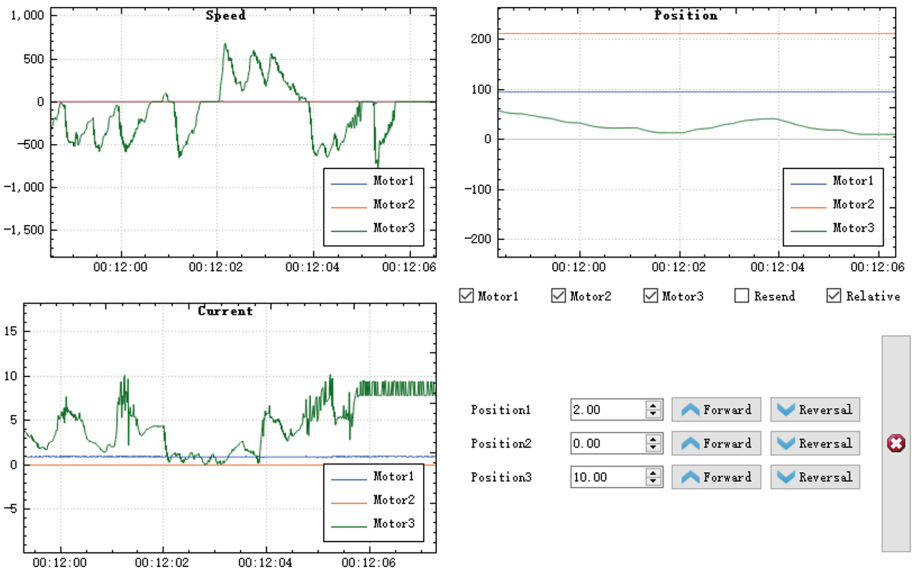

Fig. 11. The motion feedback curves of the single joint

According to the above test results and the simulation results in Sect. 4.1, the joint module designed in this paper satisfies the performance requirements of the reconfigurable intelligent robot.

4.3 The Simulation of the Fast Self-reconfigurable Module

When the static magnetic field is used to simulate the different axial distance among the moving armature and the magnetic core seat and the magnetic conductive shell, the attractive force of electromagnet of the core component of the fast self-reconfigurable module can provide in the case of power-off, and is shown in Fig. 12.

As shown in Fig. 12, the static attraction of the electromagnet of the core component of the rapid self-reconfiguration module can fully meet the requirement of more than 500N, and the closer the moving armature is to the magnetic core, the greater the attraction.

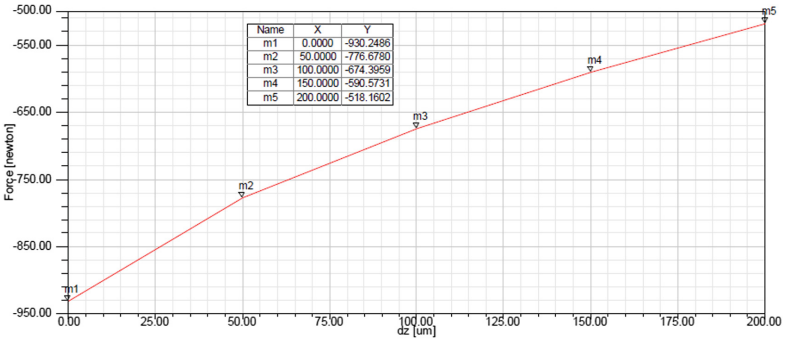

Fig. 12. The curve of electromagnet attractive force with spacing

5 Conclusions

This paper designed and implemented a reconfigurable intelligent robot. First, the topology of the reconfigurable intelligent robot is determined by the topology analysis of the bionic robot. After the kinematics modeling of the reconfigurable intelligent robot, the performance parameters of the robot joint module are obtained. In addition, through the reconfigurable intelligent robot gait planning simulation to confirm the range of motion of the joints of the robot, the speed of motion, and the maximum torque of motion. On this basis, the paper completed the software and hardware scheme design and rapid self-reconfiguration module design of the robot joint module. Finally, the experimental results show that the design indicators meet the performance requirements of reconfigurable intelligent robots.

Acknowledgments. This work was partially supported by the National Natural Science Foundation of China (No. U1813216 and No. 61803221), the Science and Technology Research Foundation of Shenzhen (JCYJ20160301100921349 and JCYJ20170817152701660). The author is thankful to several brilliant engineers, including: Xingzhang Wu, Guanyu Wang (HIT), Ruiping Zhao, Xun Ran, and Shuanglong Li, Jing Xiao for providing support and necessary facilities.

References

1. Will, P., Castano, A., Shen, W.-M.: Robot modularity for self-reconfiguration. In: Proceedings of SPIE Sensor Fusion and Decentralized Control in Robotic Systems II, vol. 3839, pp. 236–245 (1999)
2. Suh, J.W., Homans, S.B., Yim, M.: Telecubes: mechanical design of a module for a self-reconfigurable robotics. In: International Conference on Robotics and Automation, pp. 4095–4101. IEEE, Washington DC (2002)
3. Kotay, K., Rus, D., Vona, M., McGray, C.: The self-reconfiguring robotic molecule: design and control algorithms. In: Algorithmic Foundations of Robotics (1998)
4. Murata, S., Kurokawa, H., Yoshida, E., Tomita, K., Kokaji, S.: A 3-D self-reconfigurable structure. In: 1998 IEEE International Conference on Robotics and Automation, pp. 432–439. IEEE, Leuven (1998)

5. Rus, D., Vona, M.: Self-reconfiguration planning with compressible unit modules. In: 1999 IEEE International Conference on Robotics and Automation, pp. 2513–2520. IEEE, Detroit (1999)
6. Yim, M., Zhang, Y., Roufas, K., Duff, D., Eldershaw, C.: Connecting and disconnecting for chain self-reconfiguration with PolyBot. IEEE/ASME Trans. Mechatron. **7**, 442–451 (2000)
7. Yim, M., Duff, D.G., Roufas, K.D.: PolyBot: a modular reconfigurable robot. In: IEEE International Conference on Robotics and Automation, pp. 514–520. IEEE, San Francisco (2000)
8. Zhang, Y., Roufas, K., Eldershaw, C., Yim, M., Duff, D.: Sensor computations in modular self reconfigurable robots. In: Siciliano, B., Dario, P. (eds.) Experimental Robotics VIII. STAR, vol. 5, pp. 276–286. Springer, Heidelberg (2003). https://doi.org/10.1007/3-540-36268-1_24
9. Guan, X., Zheng, H., Zhang, X.: Biologically inspired quadruped robot biosbot: modeling, simulation and experiment. In: 2nd International Conference on Autonomous Robots and Agents, pp. 261–266. IEEE, Palmerston North (2004)
10. Hayashi, I., Iwatsuki, N., Iwashina, S.: The running characteristics of a screw-principle microrobot in a small bent pipe. In: Sixth International Symposium on Micro Machine and Human Science, pp. 225–228. IEEE, Nagoya (1995)
11. Arikawa, K., Hirose, S.: Development of quadruped walking robot TITAN-VIII. In: IEEE/RSJ International Conference on Intelligent Robots and Systems, pp. 208–214. IEEE, Osaka (1996)
12. Denavit, J., Hartenberg, R.: A kinematic notation for lower-pair mechanisms based on matrices. Trans. ASME J. Appl. Mech. **23**, 215–221 (1955)
13. Park, F.C., Kim, M.W.: Lie theory, Riemannian geometry, and the dynamics of coupled rigid bodies. Zeitschrift fur angewandte Mathematik und Physik ZAMP **51**(5), 820–834 (2001)
14. Mladenova, C.D.: Group-theoretical methods in manipulator kinematics and symbolic computations. J. Intell. Syst. **8**(1), 21–34 (1993)
15. Craig, J.J.: Inroduction to Robotics, 3rd edn. China Machine Press, Beijing (2005)
16. The Kollmorgen Torquer Brushless Motor Series direct drive frameless motor. https://www.kollmorgen.com/en-us/products/motors/direct-drive/tbm-series/
17. The Leaderdriver LHSG-I Series harmonic reducer. http://www.leaderdrive.om/product.-hp?id=21
18. Li, J., Tan, Q., Zhang, Y., Zhang, K.: Study on the calculation of magnetic force based on the equivalent magnetic charge method. In: 2012 International Conference on Applied Physics and Industrial Engineering, Physics Procedia, pp. 190–197 (2012)
19. STMicroelectroincs, STM32F103 devices use the Cortex-M3 core, with a maximum CPU speed of 72 Mhz. https://www.st.com/en/microcontrollers-microprocessorsstm32f103.html
20. Hirose, S., Yoneda, K., Tsukagoshi, H.: TITAN VII: quadruped walking and manipulating robot on a steep slope. In: IEEE International Conference on Robotics and Automation, pp. 494–500. IEEE, Albuquerque (1997)